An Epitaxial Model for Heterogeneous Nucleation on Potent Substrates

ZHONGYUN FAN

In this article, we present an epitaxial model for heterogeneous nucleation on potent substrates. It is proposed that heterogeneous nucleation of the solid phase (S) on a potent substrate (N) occurs by epitaxial growth of a pseudomorphic solid (PS) layer on the substrate surface under a critical undercooling (ΔT_c). The PS layer with a coherent PS/N interface mimics the atomic arrangement of the substrate, giving rise to a linear increase of misfit strain energy with layer thickness. At a critical thickness (h_c), elastic strain energy reaches a critical level, at which point, misfit dislocations are created to release the elastic strain energy in the PS layer. This converts the strained PS layer to a strainless solid (S), and changes the initial coherent PS/N interface into a semicoherent S/N interface. Beyond this critical thickness, further growth will be strainless, and solidification enters the growth stage. It is shown analytically that the lattice misfit (f) between the solid and the substrate has a strong influence on both h_c and ΔT_c; h_c decreases; and ΔT_c increases with increasing lattice misfit. This epitaxial nucleation model will be used to explain qualitatively the generally accepted experimental findings on grain refinement in the literature and to analyze the general approaches to effective grain refinement.

DOI: 10.1007/s11661-012-1495-8

I. INTRODUCTION

SOLIDIFICATION of metallic materials usually comprises two distinct stages: nucleation and growth. However, the overwhelming majority of research has been focused on the understanding of crystal growth with the nucleation stage being under-investigated mainly because of experimental difficulties.[1]

The classical heterogeneous nucleation theory[2,3] considers the balance between the interfacial energy change and the volume free energy change during the creation of a spherical cap on the substrate, and uses contact angle as a measure of the substrate potency. The energy barrier for nucleation is surmounted stochastically by energy fluctuation in the melt, and a steady-state nucleation rate can be derived as a function of temperature by statistical analysis.[3] Hence, heterogeneous nucleation is treated as a stochastic process, which is dependent on both temperature and time. However, it is now realized that the classical heterogeneous nucleation theory is not applicable for potent nucleating substrates, where the contact angle is so small (effectively zero) that the creation of a spherical cap becomes unphysical.[4]

Heterogeneous nucleation involving potent substrates is better treated as an *athermal* and *deterministic* process, in which the number of nucleation events is determined only by the driving force, being independent of time.[5,6] This has led to the development of the free growth model for grain initiation on a potent substrate.[5] The free growth model suggests that a new crystalline phase could start growing freely, without any delay, at an undercooling inversely proportional to the diameter of the substrate, indicating that grain initiation is neither time dependent nor stochastic. This means that growth starts first on the largest particle in the melt as soon as the required undercooling is reached, followed by progressively smaller ones as the undercooling is increased. Grain size is limited by recalescence, after which no further grain initiation occurs. In addition, there have been other approaches to heterogeneous nucleation on potent substrates. The hypernucleation hypothesis[7,8] suggests that a solute-rich layer structurally similar to α-Al forms on the surface of TiB_2 particles even over the alloy liquidus, and that this layer serves as precursor for the formation of α-Al. The adsorption model[4,9] supposes that beyond a critical undercooling, a new crystalline phase forms on the substrate surface by adsorption of solute elements, and it is likely to act as a precursor for heterogeneous nucleation.

At the atomic level, the process of heterogeneous nucleation on a potent substrate can be considered to be atom-by-atom building of the initial solid phase on a template. Therefore, the lattice matching across the solid/substrate interface should play an important role in this process. Relevant to this process is epitaxial growth of a thin layer of one material on the surface of another material (the substrate), which has been the subject of intense study for many years due to the interests in fabrication of strained epitaxial layer devices for the semiconductor industry.[10] The scientific basis for epitaxial growth of strained layers on a substrate originates from the theory of Frank and Van der Merwe.[11] This theory predicts that a coherent (or

ZHONGYUN FAN, Professor and Director of BCAST, is with the Brunel Solidification Centre for Advanced Technology (BCAST), Brunel University, Uxbridge, Middlesex, UB8 3PH, U.K. Contact e-mail: Zhongyun.fan@brunel.ac.uk
Manuscript submitted April 19, 2012.
Article published online November 8, 2012

pseudomorphic) layer of a crystal can grow on a substrate with a slight lattice misfit, provided the thickness of the layer is less than a critical thickness h_c (see Figure 1). It is, therefore, of both theoretical and technological importance to be able to predict h_c as a function of lattice misfit between the epitaxial layer and the substrate. Two major approaches were proposed to analyze h_c; one is the force balance theory of Matthews and Blakeslee,[12,13] and the other is the theory of Ball and Van der Merwe[14] based on the principle of energy minimization. Both theories, as have been shown to be equivalent,[15] predict that h_c decreases sharply with increasing lattice misfit.

Interestingly, Frank and Van der Merwe's theory was applied to study heterogeneous nucleation of a solid on a crystalline substrate during solidification of a metallic melt by Turnbull and Vonnegut[16] as early as in 1952. They based their analysis on the classical heterogeneous nucleation theory,[2] which, we now know, breaks down for systems with a small contact angle,[4] such as systems where grain refinement is relevant. Nevertheless, their analysis suggests that nucleation undercooling increases sharply with increasing lattice misfit between the solid and the substrate. Further realization of the importance of lattice matching at the solid/substrate interface in more recent years has led to the development of the edge-to-edge matching approach for the identification of new substrates for grain refinement.[17,18] However, it is important to realize that it is the naturally exposed surface planes of the substrate that are relevant to heterogeneous nucleation, not the arbitrary crystallographic planes matching the solid lattice.

Another interesting phenomenon related to the subject of this article is the atomic ordering of the liquid phase at the liquid/substrate interface. Recently, it was found experimentally that the free surfaces of a number of pure liquid metals (*e.g.*, References 19,20) and some binary metallic liquids (*e.g.*, References 21,22) have a layered structure, showing a tendency to some degree of ordering. This layered structure was attributed to the hard-wall effect of an abrupt change of the electron density at the liquid/vapor interface, against which the liquid atoms were packed in layers. Subsequent to that study, the interface between liquid metal and a solid substrate (a physical hard wall) was also found experimentally to exhibit a similar layered structure. Oh *et al.*[23] studied the atomic arrangement at the interface between liquid Al and α-Al_2O_3 by high-resolution transmission electron microscopy (HRTEM) at 1123 K (850 °C). They found that there were up to six layers of partially ordered Al atoms in the liquid at the interface with a structure resembling that of α-Al_2O_3.[23,24] Theoretical studies by Hashibon *et al.*[25,26] using molecular dynamic (MD) simulation predicted that some degree of in-plane atomic ordering takes place in the liquid metal adjacent to the crystalline solid surface, and that such ordering is dependent on the structure of the substrate. More recently, Men and Fan[27] studied systematically the effect of crystallographic misfit between the substrate and the corresponding equilibrium solid on the atomic structure at the liquid/substrate interface. They found that atomic layering is independent, while the in-plane atomic ordering is strongly dependent on the lattice misfit, with the in-plane ordering increasing with decreasing lattice misfit. For potent nucleating substrates, there is good atomic matching across the interface between the substrate and the solid, and atomic ordering at temperatures above the liquidus is expected to be stronger.[27] Such atomic layering and partial in-plane ordering in the liquid at the solid/liquid interface at temperatures above the liquidus can be considered as a pre-nucleation event.

In this article, we present an epitaxial model for heterogeneous nucleation on potent nucleating substrates. Based on the description of the physical model, we conduct a quantitative analysis of the epitaxial nucleation process for deriving the critical thickness and the critical undercooling required for epitaxial nucleation. The discussion focuses on the sensitivity of the model, the potency and efficiency of the nucleating system, and the application of the epitaxial model to explain the experimentally observed phenomena of grain refinement in the literature.

II. THE EPITAXIAL NUCLEATION MODEL

A. *The Physical Model*

During solidification of a liquid (L) containing potent nucleating substrates (N) (Figure 1(a)), when the temperature falls below the liquidus to reach a critical undercooling (ΔT_c), the nucleation process starts by increasing atomic ordering in the layered structure at the L/N interface. This means that atomic ordering proceeds layer by layer, in contrast to the creation of the spherical cap of the classical heterogeneous nucleation theory. However, the initial structure of the ordered solid mimics that of the substrate rather than that of the solid to be nucleated. Following epitaxial growth conventions, this initial structure has been termed a pseudomorphic solid (PS) reflecting its structural resemblance to the substrate. The PS/N interface will be coherent at this stage. As depicted in Figure 1(b), this initial strained layer growth builds up elastic strain energy within the PS layer as the layer thickness increases. At a critical thickness, elastic strain energy reaches a critical level, rendering the pseudomorphic structure unstable. Misfit dislocations are introduced to release the elastic strain energy in the PS layer. This converts the strained PS layer to a strainless solid (S) and changes the initial coherent PS/N interface into a semicoherent S/N interface (Figure 1(c)). Beyond this critical thickness, further growth will be strainless, and solidification enters the growth stage. This process of strained growth of the pseudomorphic layer to the critical thickness is referred to as epitaxial nucleation.

In the above description, misfit dislocations were proposed as a mechanism for strain relaxation in the PS layer during the epitaxial nucleation process. However, it should be pointed out that strain relaxation, in reality, can take place through many different mechanisms, such as the formation of vacancies, stacking faults, and so on. In addition, strain relaxation may occur gradually

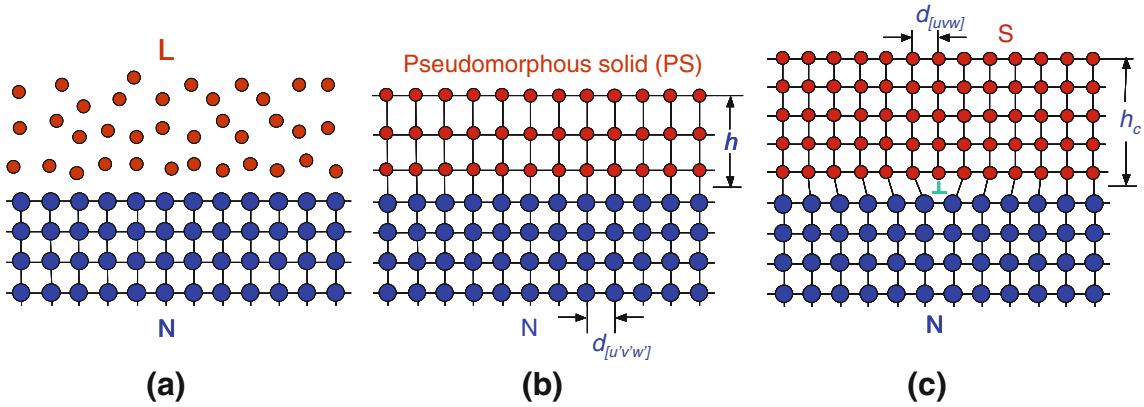

Fig. 1—Schematic illustration of the epitaxial model for heterogeneous nucleation of a solid phase (*S*) on a potent nucleating substrate (*N*) from a liquid phase (*L*) under $\Delta T > \Delta T_c$: (*a*) sketch showing the *L*/*N* interface before the growth of the *PS* layer ($h = 0$); (*b*) the initial formation of the pseudomorphic solid (*PS*) with a coherent *PS*/*N* interface; and (*c*) completion of the epitaxial nucleation at a critical thickness (h_c) by creation of misfit dislocations at the *S*/*N* interface to change the *PS* layer into the solid and to convert the coherent *PS*/*N* interface to a semicoherent *S*/*N* interface.

during the strained growth of the *PS* layer, rather than taking place at the critical thickness. As will be presented in later sections, for conceptual simplicity and convenience of mathematical treatment, we will adopt the creation of misfit dislocations at the critical thickness as the mechanism for strain relaxation.

B. *The Mathematical Analysis*

1. *Misfit strain energy in the PS layer*

For a potent nucleating substrate, the *S*/*N* interface is expected to be coherent or semicoherent. This means that there will be a well-defined crystallographic orientation relationship (OR) between the substrate and the solid. This OR is normally defined as a close packed or nearly close packed direction on a close packed plane of the solid being parallel to its counterpart of the substrate:

$$(hkl)[uvw]_S // (h'k'l')[u'v'w']_N \qquad [1]$$

It is important to point out that $(h'k'l')[u'v'w']_N$ is usually fixed and corresponds to the naturally exposed surfaces of a given nucleating particle. In contrast, $(hkl)[uvw]_S$ can be any suitable direction on a suitable plane as long as the lattice misfit is minimized at the *S*/*N* interface.

The lattice misfit (*f*) across the *S*/*N* interface can then be defined as

$$f = \frac{d_{[uvw]} - d_{[u'v'w']}}{d_{[uvw]}} \qquad [2]$$

where $d_{[uvw]}$ and $d_{[u'v'w']}$ are the atomic spacings along the close packed directions on the close packed planes of the solid and the substrate, respectively. If *f* is small, then the initial formation of the solid on the substrate will be pseudomorphic, namely, the initial solid will mimic the crystal structure of the substrate. As, in conventional solidification, the elastic modulus of the substrate (usually a ceramic) is much larger than that of the metallic solid phase, it is assumed that the lattice misfit will be accommodated only in the pseudomorphic layer in the form of elastic strain energy, which is linearly proportional to the layer thickness (*h*):[28]

$$E_S = Bf^2h, \qquad [3]$$

where the elastic constant *B* is a function of the shear modulus (μ) and the Poisson's ratio (υ):

$$B = \frac{2\mu(1+\upsilon)}{1-\upsilon}. \qquad [4]$$

In general, both the elastic constant *B* and the lattice misfit *f* are functions of temperature, and their values should be taken for the appropriate temperature concerned.

2. *Energy of misfit dislocations*

The misfit strain energy E_s increases linearly with the layer thickness *h*. At a critical thickness h_c, the pseudomorphic structure becomes unstable, and misfit dislocations are created at the *S*/*N* interface, resulting in the release of the elastic strain energy in the *PS* layer. According to dislocation theory,[29] the energy of a dislocation (edge type) per unit length (E'_D) is given by

$$E'_D = Db^2\left(\ln\frac{h_c}{b} + 1\right) \qquad [5]$$

And

$$D = \frac{\mu}{4\pi(1-\upsilon)}, \qquad [6]$$

where *D* is a constant for the solid phase, and *b* is the magnitude of the Burger's vector of the misfit dislocations. For isotropic materials with two orthogonal arrays of straight dislocations lying on the interface, the total length of dislocations will be $2/S$ per unit area, where *S* is the dislocation spacing. Thus, the total dislocation energy per unit area (E_D) is

$$E_D = 2D\delta b(\ln\frac{h_c}{b} + 1) \quad [7]$$

and

$$\delta = \frac{b}{S}, \quad [8]$$

where δ is the elastic strain released by the misfit dislocations. The total energy in the pseudomorphic layer, E_T, is the sum of the unreleased elastic strain energy and the dislocation energy (E_D):

$$E_T = B(f-\delta)^2 h_c + 2D\delta b(\ln\frac{h_c}{b} + 1). \quad [9]$$

For simplicity, we assume that all the strain energy is released by the misfit dislocations; hence $\delta = f$, and

$$E_D = 2Dfb(\ln\frac{h_c}{b} + 1). \quad [10]$$

The strain energy of a dislocation is concentrated within the dislocation core, which usually has a radius of $4b$.[29] As it is not possible to overlap dislocation cores, the theoretical limit of dislocation spacing at the S/N interface is $8b$. This gives a theoretical upper limit for the lattice misfit $f_{max} = 1/8 = 12.5$ pct, which is very close to the empirical suggestion of $f_{max} = 10$ pct.[30]

3. *The critical thickness h_c*

The critical thickness h_c is defined as a thickness at which the elastic strain energy (E_S) equals the dislocation energy (E_D) by assuming the complete relaxation of the strain energy by misfit dislocations. This gives

$$Bf^2 h_c = 2Dbf\ln(\frac{h_c}{b} + 1). \quad [11]$$

where h_c delineates the epitaxial nucleation (strained layer growth) process ($0 \le h \le h_c$) and the strainless growth process ($h > h_c$). It is therefore clear that h_c is a physical property of the nucleation system comprising the substrate and the melt. This means that h_c is a function of misfit f (Eq. [11]) and is independent of solidification conditions. Unfortunately, h_c cannot be expressed as an explicit function of f. The dependence of h_c on f can be obtained numerically and is presented in Figure 2 for both Al and Mg systems. Figure 2 shows that h_c decreases sharply with increasing f for both systems. This means that smaller f leads to slower build-up of misfit strain energy, and consequently a larger critical thickness (h_c).

There is a critical lattice misfit (f_c) for epitaxial nucleation, *i.e.*, where h_c equals 1 atomic layer, beyond which epitaxial growth becomes impossible. Using the data in Table I,[31,32] from Eq. [11], one obtains $f_c = 5.7$ pct for the Al systems and $f_c = 5.8$ pct for the Mg system. The critical limit f_c is much smaller than the upper limit (12.5 pct) determined previously by the dislocation spacing.

4. *Interfacial energies*

Figure 3 presents schematically the energy status at different stages of the epitaxial nucleation process.

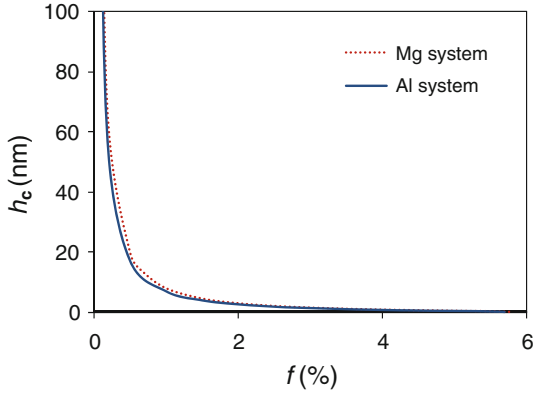

Fig. 2—The calculated critical thickness (h_c) for epitaxial nucleation from Eq. [11] as a function of misfit f. The solid line is for the Al-system and dotted line for the Mg-system.

Before the formation of the *PS* layer (Figure 3(a)), there is only one interface, *i.e.*, the L/N interface with an interfacial energyγ_{LN}. During the formation of the *PS* layer, there are two interfaces: the *PS*/L interface, ($\gamma_{PS/L}$) and the coherent *PS*/*N* interface ($\gamma_{PS/N}$) (Figure 3(b)). Once misfit dislocations are created, the *PS*/L interface becomes the L/S interface (γ_{LS}) and the *PS*/*N* interface becomes the S/N interface (Figure 3(c)) with an interfacial energy given by the sum of $\gamma_{PS/N}$ and E_D:

$$\gamma_{SN} = \gamma_{PS/N}(h_c) + 2Dfb(\ln\frac{h_c}{b} + 1), \quad [12]$$

where $\gamma_{PS/N}$ and E_D represent the chemical and structural contributions toγ_{SN},, respectively. In addition, it is assumed that the change of total interfacial energy ($\Delta\gamma$) varies linearly with h during the growth of the *PS* layer ($0 \le h \le h_c$) (Figure 4) and becomes constant when $h > h_c$. Thus, one has

$$\Delta\gamma(h) = \frac{\gamma_{LS} + \gamma_{PS/N}(h_c) - \gamma_{LN}}{h_c} h \quad (0 \le h \le h_c) \quad [13]$$

$$\Delta\gamma(h) = \gamma_{LS} + \gamma_{PS/N}(h_c) - \gamma_{LN} \quad (h > h_c). \quad [14]$$

It is important to point out that all the interfacial energies here are specific to the relevant crystallographic planes, and that they should not be confused with those used in the literature, which are usually nonspecific to crystallographic orientation.

5. *Heterogeneous nucleation of the solid phase*

The energy changes of growth of the *PS* layer are illustrated schematically in Figure 4 as a function of the layer thickness h. The strain energy E_S increases linearly with h and becomes a constant (E_D) when $h > h_c$; the interfacial energy change $\Delta\gamma$ varies linearly with h and becomes constant, when $h > h_c$; the volume free energy change also changes linearly with h. This gives $\Delta G = 0$ for $0 \le h \le h_c$ and a linearly decreasing ΔG when $h > h_c$. According to such description, the total free energy change (ΔG_T) for isothermal transformation of a layer of liquid with a thickness of h_c and a cross-sectional area of

Table I. Summary of the relevant physical properties at 933 K (660 °C) for Al and 923 K (650 °C) for Mg

Symbol	Definition	Value	Unit	Ref
b	Burger's vector of Al	2.9141×10^{-10}	m	[a]
	Burger's vector of Mg	3.2650×10^{-10}		[a]
μ	shear modulus of Al	16.2×10^{9}	N m^{-2}	[31][b]
	shear modulus of Mg	10.6×10^{9}		[32][b]
υ	Poisson's ratio of Al	0.369	–	[31][b]
	Poisson's ratio of Mg	0.350		[32][b]

[a] b is assumed to be the atomic spacing along the close packed direction on the close packed plane of the solid.
[b] both μ and υ are calculated from the experimental data at temperatures below 773 K (500 °C)[31,32] by linear extrapolation.

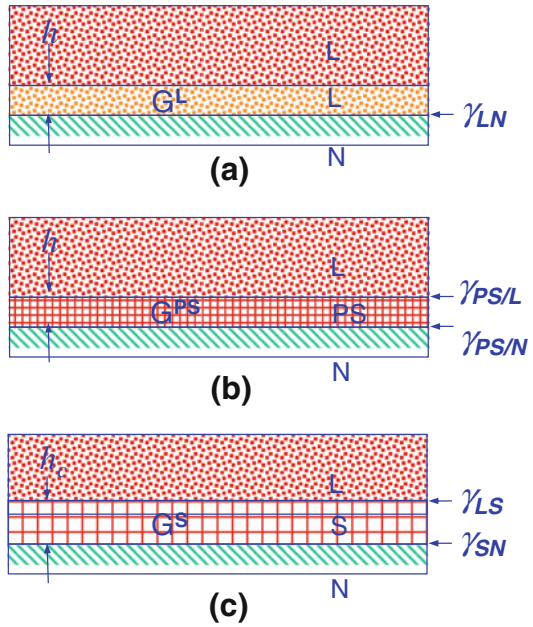

Fig. 3—Schematic illustration of the energy status at different stages of epitaxial nucleation under $\Delta T > \Delta T_c$: (*a*) before; (*b*) during; and (*c*) after the epitaxial nucleation process.

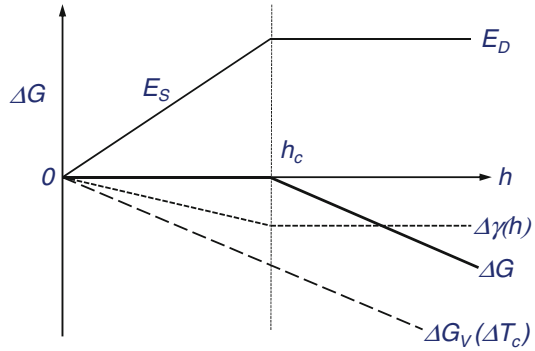

Fig. 4—Schematic illustration of the change in the various energies as a function of the layer thickness (h) during epitaxial nucleation under a critical undercooling (ΔT_c). The critical thickness h_c is defined as the thickness at which point the strain energy (E_S) equals the dislocation energy (E_D). When $0 \le h \le h_c$, the epitaxial growth of the *PS* layer continues to the critical thickness (h_c), at which the volume free energy change (ΔG_V), the interfacial energy change ($\Delta\gamma$), and the strain energy (E_S) are balanced ($\Delta G = 0$). When $h > h_c$, the solidification enters the growth stage.

A into a *PS* layer of the same dimension can be described by the following equation:

$$\Delta G_T = G^{PS} h_c A + \gamma_{L/PS} A + \gamma_{PS/N} A - G^L h_c A - \gamma_{LN} A. \quad [15]$$

As $G^{PS} = G^S + Bf^2$ and $G^S - G^L = -\Delta S_V \Delta T$ for a small undercooling ΔT_c, from Eqs. [13] and [15], one obtains the free energy change per unit area (ΔG) as shown in Figure 4:

$$\Delta G = -\Delta S_V \Delta T h_c + Bf^2 h_c + \Delta\gamma(h_c) \quad [16]$$

where ΔS_V is the entropy of fusion per unit volume. As $\Delta G = 0$ at $h = h_c$, from Eq. [16] one has

$$\Delta T_c = \frac{Bf^2 h_c + \Delta\gamma(h_c)}{\Delta S_V h_c}. \quad [17]$$

Inserting Eqs. [11], [12], and [13] into Eq. [17], one obtains

$$\Delta T_c = \frac{\gamma_{LS} + \gamma_{SN} - \gamma_{LN}}{\Delta S_V h_c}. \quad [18]$$

It is to be noted that all the interfacial energy terms in Eq. [18] are functions of the misfit f. For a given misfit f, Eq. [18] offers the critical undercooling (ΔT_c) under which the *PS* layer is able to grow to the critical thickness h_c (Figure 2).

It is clear from the previous analysis that the critical undercooling (ΔT_c) is the minimum undercooling required for epitaxial nucleation. When $\Delta T < \Delta T_c$, there is no *PS* layer as the growth of the *PS* layer will increase ΔG. However, when $\Delta T > \Delta T_c$, the *PS* layer will grow continuously beyond the critical thickness h_c with $\Delta G < 0$ for all h, as illustrated schematically in Figure 5. This means that epitaxial nucleation is a deterministic process and is only dependent on the actual undercooling relative to the critical undercooling. If $\Delta T \le \Delta T_c$, then there is no nucleation, and if $\Delta T > \Delta T_c$, then nucleation will take place. This is in contrast to the classical nucleation process, which is a stochastic process where the creation of nuclei relies on energy fluctuation.

Equations [17] and [18] show that ΔT_c is a function of lattice misfit f, although the dependence of ΔT_c on f

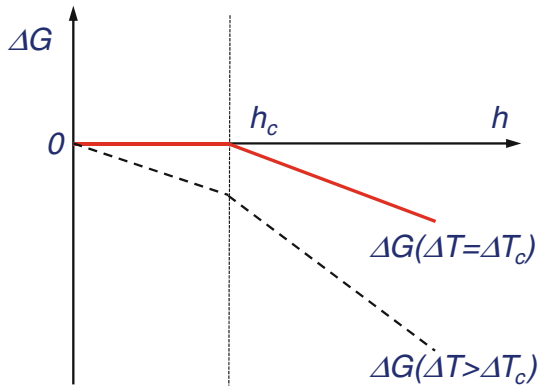

Fig. 5—Schematic illustration of the free energy change (ΔG) as a function of the layer thickness (h) during epitaxial nucleation under different undercoolings (ΔT) relative to the critical undercooling (ΔT_c). Solid line for $\Delta T = \Delta T_c$; and dashed line for $\Delta T > \Delta T_c$. It is impossible to grow the *PS* layer when $\Delta T < \Delta T_c$ as $\Delta G > 0$.

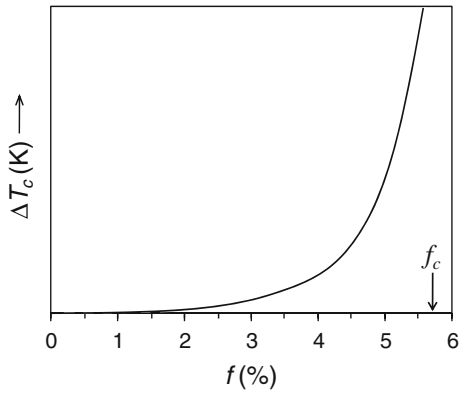

Fig. 6—Schematic illustration of the critical undercooling (ΔT_c) for epitaxial nucleation as a function of misfit f. ΔT_c increases with increasing f, and becomes very large when f approaches the critical misfit f_c.

cannot be explicitly evaluated because of the lack of a complete set of interfacial energy data. Simple analysis of Eq. [17] indicates that ΔT_c is a monotonic increasing function of f: ΔT_c is small when f is small, and becomes very large when f approaches f_c. The dependence of ΔT_c on f is illustrated schematically in Figure 6.

III. DISCUSSION

A. *Sensitivity Analysis*

1. *Effect of substrate size*

Equation [3] assumes implicitly that the substrate is infinite in both thickness and lateral dimensions.[28] In a real solidification system, the substrate always has a finite size. For instance, for grain refining Al-alloys by Al-5Ti-1B master alloy, the active TiB_2 substrates have a size of around 1 μm.[33] It is therefore important to analyze the applicability of the epitaxial model to finite substrate size.

For a conventional pseudomorphic structure created by epitaxial growth, the elastic strain is predominately in the pseudomorphic layer because the substrate is too thick to be compliant.[15] However, for thin substrates the elastic energy is more evenly distributed between the pseudomorphic layer and the substrate so that the total energy is reduced. This means that some of the elastic strain energy may be transferred to the substrate (strain transfer), and consequently the original lattice misfit is reduced because of the finite substrate size (strain dilution). This strain dilution effect has been analyzed in the case of epitaxial growth of semiconductors by the introduction of a strain dilution factor $\phi_l (\phi_l > 1)$:[34]

$$\phi_l = \frac{f}{f'}, \qquad [19]$$

where f is the original lattice misfit calculated from the crystallographic data of the system, and f' is the elastic strain in the thin film on a finite substrate. By assuming that both the thin film and the substrate have the same shear modulus, Luryi and Suhir[34] analyzed the effect of the finite lateral substrate size ($l \times l$) on the strain dilution factor ϕ_l, and found that ϕ_l decreased sharply with an increase in l/h, and with $\phi_l \approx 1$ when $l/h = 4$. Similar conclusions were obtained by Lo[35] for a finite substrate thickness and by Huang[36] for substrates with finite dimensions in 3D. Lo[35] calculated the normalized effective *PS* layer thickness as a function of the normalized substrate thickness, and concluded that for a substrate with a thickness h_N, the effect of finite substrate size could be omitted without causing significant error if $h_N/h_c > 4$.

From Figure 2, h_c = 0.8 nm for the Al/TiB_2 system, and h_c = 13.6 nm for the Mg/Zr system. The critical thickness is orders of magnitude smaller than the size of active nucleating particles, and we can therefore conclude that the epitaxial nucleation theory can be applied without consideration of the effect of limited particle size.

2. *Effect of difference in elastic moduli*

A key feature of the epitaxial nucleation model is the generation of misfit dislocations driven by the stored elastic energy in the *PS* layer. Hence, the elastic moduli of both the substrate (μ_N) and the solid (μ_S) will affect the nucleation process through their effect on the amount of stored elastic energy. Following a similar approach to Eq. [19], a strain dilution factor ϕ_μ was derived to account for the effect of elastic modulus on the epitaxial growth of semiconductors:[36]

$$\phi_\mu = 1 + \frac{h_c}{h_N}\frac{\mu_S}{\mu_N}. \qquad [20]$$

For heterogeneous nucleation of metallic solids on ceramic particles, $\mu_N \gg \mu_S$ and $h_N >> h_c$. This means that the strain dilution factor (ϕ_μ) is close to 1, suggesting that the misfit strain energy will be stored only in the metallic solid without any strain dilution by the substrate, and hence the epitaxial nucleation model can be applied to metallic alloys without considering the difference in elastic modulus between the solid and the substrate.

3. *Effect of temperature*

According to Eq. [11], for a given nucleating system, the critical layer thickness for epitaxial nucleation is simply described as a function of the elastic modulus and the lattice parameters of both the solid and the substrate. The effect of temperature on the epitaxial nucleation process can be analyzed through the temperature dependence of the elastic modulus and the lattice parameter. Recently, this has been analyzed theoretically by Ito *et al.*[37] for the epitaxial growth of semiconductors. They found that the elastic constants decrease as the lattice parameters increase with increasing temperature. However, the overall effect of temperature on the elastic strain energy accumulated in the pseudomorphic layer is rather small due to the counter effect of temperature on elastic modulus and lattice parameter. For instance, with a temperature increase of 1000 K the increase in elastic strain energy in the pseudomorphic layer is about 10 pct.[37] This means that when there is a lack of high temperature data for the elastic modulus and lattice parameter, the corresponding data for room temperature may be used without significant compromise of accuracy.

B. *Effect of Solute on Epitaxial Nucleation*

In the literature, the effect of solute elements on heterogeneous nucleation is taken into account through the phenomenon of growth restriction which allows more nucleating substrates to be active for heterogeneous nucleation before recalescence.[38] Easton and StJohn[38,39] proposed a semiempirical model based on the constitutional undercooling theory. Their analysis showed that grain size can be related closely to the growth restriction factor. In such an approach, the grain refinement due to the increased solute contents is explained by the increased nucleation events through delayed recalescence.[39] Further development in this direction has seen a better analytic approach to the solute effect[40,41] and the more recent postulation of the interdependence theory by StJohn *et al.*[42] They believe that grain formation is the result of repeated cycles of growth and nucleation events moving toward the thermal center of the casting.

The epitaxial nucleation model can provide new insights to solute effects on nucleation. According to the Gibbs adsorption rule,[43] solute atoms in the alloy melt may segregate to the L/N interface if such segregation leads to a reduction of interfacial energy. The segregated solute atoms can affect the structure of the pseudomorphic layer during the nucleation process. If the segregated element reduces the lattice misfit (f), then it will promote heterogeneous nucleation. Conversely, if a segregated element increases the lattice misfit, it will hinder heterogeneous nucleation, giving rise to a poisoning effect.

Based on the above analysis, solute elements (with a concentration X) can be divided into three categories:

- Group A: elements with $\frac{\partial \gamma_{LN}}{\partial X} < 0$ and $\frac{\partial f}{\partial X} < 0$, enhancing nucleation;
- Group B: elements with $\frac{\partial \gamma_{LN}}{\partial X} < 0$ and $\frac{\partial f}{\partial X} > 0$, poisoning nucleation;
- Group C: elements with $\frac{\partial \gamma_{LN}}{\partial X} > 0$; or $\frac{\partial f}{\partial X} = 0$, having no effect on nucleation.

In general, a reduction of the interfacial energy by segregated solute elements at the L/N interface can be achieved by

- Reaction with the solvent to form an intermetallic phase on the substrate;
- Reaction with the substrate to form a new compound on the substrate;
- Segregation at the L/N interface to influence the lattice parameter of the solid phase; and
- Dissolution into the substrate to change the lattice parameter of the substrate.

In the first two cases, a new substrate is formed through chemical reaction, and both its crystal structure and lattice parameter will be different from those of the original substrate; whereas in the latter two cases, there is no change in crystal structure on either side of the S/N interface, but the lattice parameter of either the solid or the substrate will have changed. However, the effect of a solute element on nucleation depends on how the lattice misfit at the S/N interface is changed by the solute element. A solute element enhances heterogeneous nucleation if it reduces the misfit; otherwise, a solute element will poison heterogeneous nucleation if it increases the misfit. In addition, solute elements may also reduce the tendency of agglomeration between the nucleating particles because of reduced interfacial energy at the L/N interface, providing an increased number of active nucleating particles. Theoretically, it should be possible to select a nucleating substrate and solute elements in such a way that nucleation is enhanced.

Although the epitaxial nucleation model assumes that there is no chemical reaction at the L/N interface, it is applicable to cases where chemical reaction does occur, as long as the reaction product is treated as the new substrate to replace the original substrate for the calculation of lattice misfit. After any potential chemical reaction, the new substrate will be in chemical equilibrium with the adjacent liquid phase, and the epitaxial nucleation model can be applied to the new substrate without considering any further chemical reaction.

The epitaxial nucleation model has been applied to explain some of the experimental findings on chemical inoculation of Al-alloys and Mg-alloys for grain refinement. Table II summarizes the crystallographic data and the calculated misfit for the relevant nucleating systems of interest.

TiB_2 has a lattice misfit of −4.22 pct with Al and is widely used as an effective nucleating substrate in the Al-Ti-B based grain refiners for Al-alloys.[44] In order to increase the potency of TiB_2 particles in the grain refiner alloy, excess Ti is added to form a thin layer of Al_3Ti on the TiB_2 surface.[45] This effectively replaces the original TiB_2 substrate with Al_3Ti which has an extremely small lattice misfit with α-Al (0.09 pct), resulting in enhanced grain refinement.[46] In contrast, Zr addition to TiB_2 inoculated Al-alloys will cause the conversion of TiB_2 to $(Ti_{1-x}Zr_x)B_2$ through the substitution of Ti by Zr

Table II. Summary of the crystallographic data and the calculated lattice misfit for the relevant nucleating systems at 933 K (660 °C) for Al and 923 K (650 °C) for Mg

Interface S/N	Crystal Structure, Lattice Parameters[a] (nm)	OR: $(hkl)[uvw]_S//(h'k'l')[u'v'w']_N$[b]	$d_{[u'v'w']}$ (nm)	$d_{[uvw]}$ (nm)	f (Pct)
Al/TiB_2	S: fcc, $a = 0.42112$[45] N: hcp, $a = 0.30372$, $c = 0.32368$[45]	(111)[110]// (0001)[11−20]	0.30372	0.29141	−4.22
Al/Al_3Ti	S: fcc $a = 0.42112$ N: tetragonal, $a = 0.3883$, $c = 0.8679$[51]	(111)[110]//(112)[20−1]	0.29116	0.29141	0.09
Al/ZrB_2	S: fcc $a = 0.41212$ N: hcp, $a = 0.3883$, $c = 0.8679$[52]	(111)[110]//(0001)[11−20]	0.31690	0.29141	−8.75
Mg/Zr	S: hcp, $a = 0.3265$, $c = 0.5308$[31] N: hcp, $a = 0.32431$, $c = 0.5180$[53]	(0001)[11−20]//(0001)[11−20]	0.32431	0.32650	0.67
Mg/Al_3Zr	S: hcp, $a = 0.3265$, $c = 0.5308$ N: tetragonal, $a = 0.4038$, $c = 1.7428$[54][c]	(0001)[11−20]//(114)[110]	0.28553	0.32650	12.55

[a]The lattice parameters were calculated from room temperature data from JCPDS files and the coefficients of thermal expansion given in the relevant references.

[b]The orientation relationship (OR) is obtained by assuming that the close packed direction on the close packed plane of the solid is parallel to its counterpart of the substrate.

[c]The lattice parameters for Al_3Zr are from Ref.[54] The coefficient of thermal expansion for Al_3Zr is not available but is assumed to be the same as that for Al_3Ti.[51]

because ZrB_2 is more stable than TiB_2.[47] This substitution results in an increase of the lattice misfit from −4.22 pct toward −8.75 pct (for pure ZrB_2) depending on the level of Zr addition. This renders TiB_2 particles less potent for nucleating α-Al, and explains the poisoning effect of Zr on Al-Ti-B based grain refiners.

Similarly, the epitaxial nucleation model can be used to explain the powerful grain refining effect of Zr on α-Mg and the poisoning effect of Al on Zr in Al-containing Mg-alloys. As shown in Table II, Zr and Mg have the same crystal structure and similar lattice parameters. The lattice misfit between Zr and Mg at 923 K (650 °C) is only 0.67 pct, making Zr an extremely potent nucleating substrate for α-Mg.[48] However, for Mg-alloys containing Al as a solute element, Al will react with Zr forming on the surface of the Zr particles a layer of Al_3Zr intermetallic, which has a large lattice misfit of 12.55 pct with α-Mg, making Zr particles inactive for heterogeneous nucleation.[49]

C. *Enhancing Heterogeneous Nucleation for Grain Refinement*

Grain refinement by chemical inoculation can be achieved by increasing both the nucleation *potency* and the grain initiation *efficiency*. In describing grain refinement, "potency" and "efficiency" have been frequently used in the literature in a way creating very much confusion. It is necessary to define nucleation potency, grain initiation efficiency and effective grain refinement.

Nucleation potency is defined as the degree of the lattice matching at the S/N interface during heterogeneous nucleation. Lattice misfit f can be used as a quantitative measure of the nucleation potency, and the smaller the lattice misfit, the higher the nucleation potency. Therefore, nucleating potency is an inherent physical property of a given nucleating system, which consists of the substrate and the liquid. Nucleation potency refers to the ease of the formation of the solid phase on a given nucleating particle in the liquid phase. It depends on neither the physical state of the solid particles (such as number density, size, and size distribution) nor the solidification conditions (*e.g.*, cooling rate).

Grain initiation efficiency is defined as the fraction of the particles participating in grain initiation out of the total number of available particles during the entire solidification process. It is clear from this definition that grain initiation efficiency is a function of the specific physical characteristics of both the nucleating particles and solidification conditions, such as number density, size, size distribution of the nucleating particles, as well as cooling rate. For a given nucleating system, nucleation potency is fixed but grain initiation efficiency can be changed by modifying the physical characteristics of the nucleating particles and/or changing the solidification conditions.

Effective grain refinement refers to the scale of the solidified microstructure. Average grain size can be used as a quantitative measure of effective grain refinement. Theoretically, effective grain refinement requires effective grain initiation, *i.e.*, a large number of grain initiation events per unit volume during solidification. Hence, effective grain refinement not only requires that the nucleating particles are sufficient in number, well dispersed, and of suitable particle size and size distribution, but also that the solidification conditions are set in such a way that solidification undercooling is maximized to allow more nuclei to initiate grains.

Liquid alloys always contain endogenous particles, such as oxides, carbides, nitrides, and various intermetallic particles. Such *in situ*-formed particles are collectively referred to as endogenous particles. Exogenous particles are introduced into the alloy melt through grain refiner addition, such as TiB_2 particles in the Al-5Ti-1B grain refiners. During solidification processing, the exogenous particles from the grain refiner are in direct competition with the endogenous particles. If the endogenous particles have higher nucleation potency

and higher grain initiation efficiency, then they will dominate the grain initiation process, leaving the exogenous particles redundant. This means that the addition of grain refiners can only be effective for grain refinement if there are no more powerful solid particles inside the melt. For instance, it is well known that conventional Al-5Ti-1B grain refiner is not effective for refining Al-Mg-based alloys (Mg > 1 wt pct). This can be explained by the competition between endogenous oxide particles and the exogenous TiB_2 particles. It has been confirmed that Al-Mg alloys contain large numbers of $MgAl_2O_4$ particles, which are naturally well dispersed, of suitable size (0.5 to 1 μm), and exhibit a narrow size distribution.[50] $MgAl_2O_4$ particles have a smaller lattice misfit with α-Al (1.4 pct), and could dominate the grain initiation process, leaving the exogenous TiB_2 particles little chance to participate in the grain initiation process thus having little effect on grain refinement.

D. *Epitaxial Nucleation Model in Relation to Other Nucleation Theories*

Classical nucleation theory[2,3] is based on a statistical analysis of the formation of atomic clusters (or spherical caps in the case of heterogeneous nucleation) with a critical radius r^*, which is thermally activated, and therefore a stochastic process. The critical undercooling (ΔT_{cn}) required to overcome the energy barrier to nucleation is given by the following equation:

$$\Delta T_{cn} = \frac{2\gamma_{LS}}{\Delta S_V r^*}. \quad [21]$$

Greer *et al.*[5] identified that a nucleated crystal can only grow freely if the free growth barrier is overcome at a critical undercooling (ΔT_{fg}), which is given by the following equation:

$$\Delta T_{fg} = \frac{2\gamma_{LS}}{\Delta S_V r}, \quad [22]$$

where r is the radius of the nucleating surface of the substrate. The free growth model has been used successfully to analyze grain initiation,[5,33] which is believed to be a deterministic process that does not require thermal activation.

The epitaxial nucleation model is only concerned with the atomistic mechanisms of the initial formation of the solid phase. Although there is no energy barrier, epitaxial nucleation does require a critical undercooling (ΔT_c) for the PS layer to grow to the critical thickness (h_c). Similar to the free growth criterion for grain initiation, epitaxial nucleation is a deterministic process. This means epitaxial nucleation becomes a "yes/no" question depending on whether the actual undercooling reaches the critical undercooling. In contrast to the classical nucleation theory, it does not require thermal activation.

However, it should be pointed out that a successful nucleation event will result in a nucleus, but may not necessarily lead to a successful grain initiation depending on whether the free growth criterion is satisfied.

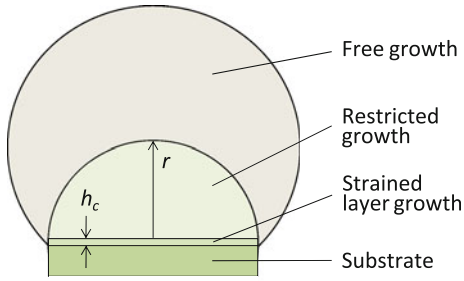

Fig. 7—Schematic illustration of epitaxial nucleation (strained layer growth) in relationship to the hemisphere created by restricted growth (grain initiation) followed by free growth.

In general, effective grain refinement requires both successful nucleation and grain initiation. If $\Delta T_{fg} > \Delta T_c$, then grain initiation becomes the controlling factor for grain refinement; otherwise, if $\Delta T_{fg} < \Delta T_c$, then nucleation will be the controlling factor. The relationship between epitaxial nucleation and grain initiation for a potent substrate with a reasonable size is depicted schematically in Figure 7. A small undercooling (ΔT_c) is required to allow the strained layer growth (epitaxial nucleation) for the creation of the initial solid layer of thickness h_c against the increasing elastic strain energy. Further undercooling is still needed to overcome the free growth barrier (curvature effect) for the hemisphere formation on the substrate if $\Delta T > \Delta T_{fg}$. Further growth beyond the hemisphere will be free (*i.e.*, free growth), resulting in the formation of a new grain.

IV. SUMMARY

An epitaxial nucleation model has been developed to describe the atomistic mechanisms of heterogeneous nucleation on a potent substrate. It is proposed that, beyond a critical undercooling, heterogeneous nucleation on a potent substrate takes place by epitaxial growth of a pseudomorphic layer on the surface of the substrate. The solid phase is formed by creating misfit dislocations at the PS/N interface to transform the pseudomorphic layer into the solid phase and the initially coherent PS/N interface to a semicoherent S/N interface. It is shown analytically that both the critical undercooling and the critical thickness for epitaxial nucleation are closely related to the lattice misfit at the S/N interface. The epitaxial nucleation model has been used to explain successfully the generally accepted experimental findings on grain refinement in the literature. In addition, we have analyzed the approaches to effective grain refinement. Effective grain refinement depends on both successful nucleation and efficient grain initiation. The nucleating particles in the grain refiner (exogenous particles) need to be highly potent (small lattice misfit), well dispersed, and of sufficient number density and of suitable size and size distribution. As endogenous solid particles, such as oxides, nitrides, carbides, and intermetallic compounds inevitably exist in alloy melts, exogenous nucleating particles are in direct competition with such endogenous particles, with the more powerful particles dictating the final grain size. Another important factor for grain

refinement is the alloy composition. Solute elements affect not only the nucleation potency by adsorption of solute elements at the L/N interface, but also grain initiation efficiency through growth restriction. Thus, effective grain refinement may be achieved by manipulation of the interaction between the solid particles (either exogenous or endogenous) and the solute elements in such a way that both nucleation potency and grain initiation efficiency are increased.

ACKNOWLEDGMENTS

The author wishes to thank Dr H. Men, Professor J.D. Hunt, and Professor A.L. Greer for their helpful and inspiring discussions on the contents of this article, and Dr Y. Wang for his help with the preparation of the crystallographic data used in the calculations. The author is grateful to the E*PS*RC for supporting the E*PS*RC Centre—LiME under Grant EP/H026177/1.

REFERENCES

1. J.A. Dantzig and M. Rappaz: *Solidification*, CRC Press, Lausanne, 2009.
2. M. Volmer and A. Webber: *Z. Phys. Chem.*, 1926, vol. 119, pp. 277–301.
3. K.F. Kelton and A.L. Greer: *Nucleation in Condensed Matter*, Elsevier, Oxford, 2011.
4. B. Cantor: *Phil. Trans. R. Soc. Lond. A*, 2003, vol. 361, pp. 409–17.
5. A.L. Greer, A.M. Bunn, A. Tronche, P.V. Evans, and D.J. Bristow: *Acta Mater.*, 2000, vol. 48, pp. 2823–35.
6. T.E. Quested and A.L. Greer: *Acta Mater.*, 2005, vol. 53, pp. 2683–92.
7. G.P. Jones and J. Pearson: *Metall. Trans. B*, 1976, vol. 7B, pp. 223–34.
8. G.P. Jones:, in *Solidification Processing*, J. Beech and H. Jones, eds., The Institute of Metals, London, 1987, p. 496.
9. W.T. Kim and B. Cantor: *Acta Metall. Mater.*, 1994, vol. 42, pp. 3115–27.
10. M. Ohring: *Materials Science of Thin Films*, 2nd ed., Academic Press, San Diego, 2002.
11. F.C. Frank and J.H. Van der Merwe: *Proc. R. Soc. Lond. A*, 1949, vol. 198, pp. 216–25.
12. J.W. Matthews and A.E. Blakeslee: *J. Cryst. Growth*, 1974, vol. 27, pp. 118–25.
13. J.W. Matthews:, in *Epitaxial Growth Part B*, J.W. Matthews, ed., Academic Press, New York, 1975.
14. C.A.B. Ball and J.H. Van der Merwe:, in *Dislocations in Solid*, F.R.N. Nabarro, ed., North Holland, Amsterdam, 1974.
15. S.C. Jain, A.H. Harker, and R.A. Cowley: *Phil. Mag. A*, 1997, vol. 75, pp. 1461–515.
16. D. Turnbull and B. Vonnegut: *Indus. Eng. Chem.*, 1952, vol. 44, pp. 1292–98.
17. M.X. Zhang, P.M. Kelly, M.A. Easton, and J.A. Taylor: *Acta Mater.*, 2005, vol. 53, pp. 1427–38.
18. M.X. Zhang, P.M. Kelly, M. Qian, and J.A. Taylor: *Acta Mater.*, 2005, vol. 53, pp. 3261–70.
19. O.M. Magnussen, B.M. Ocko, M.J. Regan, P.S. Penanen, P.S. Pershan, and M. Deutsch: *Phys. Rev. Lett.*, 1995, vol. 74, pp. 4444–7.
20. M.J. Regan, E.H. Kawamoto, S. Lee, P.S. Pershan, N. Naskil, M. Deutsch, O.M. Magnussen, B.M. Ocko, and L.E. Berman: *Phys. Rev. Lett.*, 1995, vol. 75, pp. 2498–501.
21. O.G. Shpyrko, A.Y. Grigoriev, R. Streitel, D. Pontoni, P.S. Pershan, M. Deutsch, B.M. Ocko, M. Meron, and B. Lin: *Phys. Rev. Lett.*, 2005, vol. 95, p. 106103.
22. O.G. Shpyrko, R. Streitel, V.S.K. Balagurusamy, A.Y. Grigoriev, M. Deutsch, B.M. Ocko, M. Meron, B. Lin, and P.S. Pershan: *Science*, 2006, vol. 313, pp. 77–80.
23. S.H. Oh, Y. Kauffmann, C. Scheu, W.D. Kaplan, and M. Rühle: *Science*, 2005, vol. 310, pp. 661–3.
24. S.H. Oh, C. Scheu and M. Rühle: *Korean J. Electron Microscopy,* 2006, Special Issue 1, pp. 19–24.
25. A. Hashibon, J. Adler, M.W. Finnis, and W.D. Kaplan: *Comput. Mater. Sci.*, 2002, vol. 24, pp. 443–52.
26. A. Hashibon, J. Adler, M.W. Finnis, and W.D. Kaplan: *Interface Sci.*, 2001, vol. 9, pp. 175–81.
27. H. Men and Z. Fan: *IOP Conf. Series: Mater. Sci. Eng.*, 2011, vol. 27, p. 012007.
28. J.W. Cahn: *Acta Metall.*, 1962, vol. 10, pp. 179–83.
29. D. Hull and D.J. Bacon: *Introduction to Dislocations*, 3rd ed., Pergamon Press, Oxford, 1984.
30. A. Trampert and K.H. Ploog: *Cryst. Res. Technol.*, 2000, vol. 35, pp. 793–806.
31. J.A. Brammer and C.M. Percival: *Exp. Mech.*, 1970, vol. 10, pp. 245–50.
32. *Magnesium and Magnesium Alloys*, 3rd ed., M.M. Avedesian, and H. Baker, eds., ASM International, Warrendale, PA, 1999.
33. T.E. Quested and A.L. Greer: *Acta Mater.*, 2004, vol. 52, pp. 3859–68.
34. S. Luryi and E. Suhir: *Appl. Phys. Lett.*, 1986, vol. 49, pp. 140–2.
35. Y.H. Lo: *Appl. Phys. Lett.*, 1991, vol. 59, pp. 2311–3.
36. F.Y. Huang: *Phys. Rev. Lett.*, 2000, vol. 85, pp. 784–7.
37. T. Ito, T. Araki, T. Akiyama, and K. Nakamura: *J. Cryst. Growth*, 2007, vols. 301–302, pp. 62–6.
38. M.A. Easton and D.H. StJohn: *Metall. Mater. Trans. A*, 1999, vol. 30A, pp. 1613–23.
39. M.A. Easton and D.H. StJohn: *Acta Mater.*, 2001, vol. 49, pp. 1867–78.
40. M.A. Easton and D.H. StJohn: *Metall. Mater. Trans. A*, 2005, vol. 36A, pp. 1911–20.
41. M. Qian, P,. Cao, M.A. Easton, S.D. McDonald, and D.H. StJohn: *Acta Mater.*, 2010, vol. 58, pp. 3262–70.
42. D.H. StJohn, M. Qian, M.A. Easton, and P. Cao: *Acta Mater.*, 2011, vol. 59, pp. 4907–21.
43. J. Gibbs: *The Collected Works of J. Willard Gibbs*, Langman, Green and Co, New York, 1928, vol. 1.
44. B.S. Murty, S.A. Kori, and M. Chakraborty: *Inter. Mater. Rev.*, 2002, vol. 47, pp. 3–29.
45. M. Johnsson and L. Eriksson: *Z. Metallkd.*, 1998, vol. 89, pp. 478–80.
46. P. Schumacher and A.L. Greer: *Mater. Sci. Eng., A*, 1994, vols. 181–182, pp. 1335–9.
47. A.M. Bunn, P. Schumacher, M.A. Kearns, C.B. Boothroyd, and A.L. Greer: *Mater. Sci. Technol.*, 1999, vol. 15, pp. 1115–23.
48. Y. Tamura, N. Kono, T. Motegi, and E. Sato: *J. Jpn. Inst. Light Met.*, 1998, vol. 48, pp. 185–9.
49. D.H. StJohn, M. Qian, M.A. Eastern, P. Cao, and Z. Hildebrand: *Metall. Mater. Trans. A*, 2005, vol. 36A, pp. 1669–79.
50. H.T. Li, Y. Wang, and Z. Fan: *Acta Mater.*, 2012, vol. 60, pp. 1528–37.
51. J.L. Smialek, M.A. Gedwill, and P.K. Brindley: *Scripta Metall. Mater.*, 1990, vol. 24, pp. 1291–6.
52. J. Tolle, R. Roucka, I.S.T. Tsong, C. Ritter, P.A. Crozier, A.V.G. Chizmeshya, and J. Kouvetakis: *Appl. Phys. Lett.*, 2003, vol. 82, pp. 2398–400.
53. J. Goldak, L.T. Lloyd, and C.S. Barrett: *Phys. Rev.*, 1966, vol. 144, pp. 478–84.
54. C. Amador, J.J. Hoyt, B.C. Chakoumakos, and D. Fontaine: *Phys. Rev. Lett.*, 1995, vol. 74, pp. 4955–8.